

Dynamic Aperture Improvement of PEP-II Lattices Using Resonance Basis Lie Generators*

Y. Yan, J. Irwin, Y. Cai, M. Donald, and Y. Nosochkov
Stanford Linear Accelerator Center
Stanford, CA 94309, U.S.A.

Abstract

To simplify the engineering efforts of implementing the PEP-II lattices, many modifications have been made to these lattices since the conceptual design report[1]. During the development and evolution of the lattices, changes in a lattice would often result in a significant reduction in the dynamic aperture. At such times, we often relied on a non-linear analysis using the one-turn resonance basis Lie generator to identify the cause of the degradation. In this paper, we will present such examples to facilitate the usage of map for diagnosing the problems in lattice design.

1 INTRODUCTION

In order to achieve the design luminosity of $3.0 \times 10^{33} \text{cm}^{-2} \text{s}^{-1}$ and maintain flexibility in optimizing the luminosity, we need to attain a low-beta value at the interaction point(IP) close to 1.5 cm for both the Low-Energy Ring(LER) and the High-Energy Ring(HER). As a consequence of this requirement, chromatic correction for strong quadrupoles near the IP become critical to minimize non-linear chromaticity and retain an adequate dynamic aperture. Many of the major revisions of the lattices[2][3] resulted from the improvement of the schemes for chromatic corrections.

Among the lattice examples, we will select three instances related with chromatic behaviour of the lattices. Through the examples, we will show how to analyze the one-turn map and how to identify the causes of inadequate dynamic aperture. First, let's establish some notations and terminologies used in analysis of maps.

2 EFFECTIVE HAMILTONIAN

There are many ways to extract a one-turn map from a given lattice. Among them, the most straight-forward method is based on the thin lens or symplectic kicking code. One simply replace the double-precision variables with the differential algebraic(DA)[4] variables in the phase vector wherever particles are tracked. In particular, in any object-oriented codes this scheme could be implemented easily since one could build a DA variable as an abstract type in the program. Then, a Taylor map would be obtained by tracking a vector

Table 1: Main PEP-II nominal parameters.

| Parameter | LER | HER |
|--|----------------------|----------------------|
| Energy, E [GeV] | 3.1 | 9.0 |
| Circumference, C [km] | 2.2 | 2.2 |
| Emittance, ϵ_x/ϵ_y [nm-rad] | 64.3/2.6 | 48.2/1.9 |
| Beta function, β_x^*/β_y^* [cm] | 37.5/1.5 | 50.0/2.0 |
| B-beam tune shift, $\xi_{0,x}/\xi_{0,y}$ | 0.03/0.03 | 0.03/0.03 |
| Synchrotron tune, μ_s | 0.03344 | 0.05207 |
| RF frequency, f_{RF} [MHZ] | 476 | 476 |
| RF voltage, V_{RF} [MV] | 5.1 | 18.5 |
| Damping time, τ_E/τ_x [ms] | 29.2/60.5 | 18.4/37.2 |
| Bunch length, σ_l [cm] | 1.0 | 1.0 |
| RMS $\delta E/E$, σ_E | 7.7×10^{-4} | 6.1×10^{-4} |
| Total current, I [A] | 2.14 | 0.99 |
| Synch. loss, U_0 [Mev/turn] | 0.77 | 3.58 |
| Luminosity, \mathcal{L} [$\text{cm}^{-2} \text{s}^{-1}$] | 3.0×10^{33} | 3.0×10^{33} |

initialized to the identity with DA variables through the lattice.

A Taylor map is symplectic up to the order of the truncation if the effects of the radiation damping and quantum excitation are ignored. Here we treat momentum derivation $\delta = dp/p$ as a parameter of the map and denote the Taylor map as[5]

$$z_f = \mathcal{M}(z_i, \delta) + O(N + 1), \quad (1)$$

where $O(N + 1)$ indicates that the Taylor map is truncated at an order of N , z_i is the initial phase-space coordinates, and z_f is the final phase-space coordinates.

Furthermore, because \mathcal{M} is symplectic we could define an effective Hamiltonian $\mathcal{H}_{\mathcal{E}\mathcal{F}\mathcal{F}}$ as

$$\mathcal{M}(\ddagger, \delta) = \mathcal{J}^{-1} \circ \mathcal{H}_i(\ddagger) \circ \mathcal{J}^{-1} \circ \mathcal{H}_{\mathcal{E}\mathcal{F}\mathcal{F}}(\ddagger, \delta), \quad (2)$$

here we use \mathcal{H} as a short notation of a Lie operator[6], which acts on a function of phase-space variables $f(z)$ through the Poisson bracket as $:\mathcal{H}(\ddagger):f(z) = \{\mathcal{H}(\ddagger), f(z)\}$. The effective Hamiltonian contains almost all information, near the origin, of single particle dynamics in the extracted lattice. In general, given a map extracted relative to a closed orbit, it can be expressed as

* Work supported by the Department of Energy under Contract No. DE-AC03-76SF00515.

$$\mathcal{H}_{\mathcal{E}\mathcal{F}\mathcal{F}}(\ddagger, \delta) = \sum_{\mathcal{N} \geq 3} \mathcal{H}_{\mathcal{N}}(\ddagger, \delta), \quad (3)$$

with

$$\mathcal{H}_l = \mu_x J_x + \mu_y J_y,$$

where μ_x and μ_y are tunes, J_x and J_y are the action invariances of the lattice, and $\mathcal{H}_{\mathcal{N}}$ are non-linear parts of the Hamiltonian. $H_{\mathcal{N}}$ could be calculated order-by-order perturbatively from the underlining Taylor map. In the next section, we will show examples of how to use the effective Hamiltonian.

3 NONLINEAR DISPERSION

One of the major revisions of the LER lattice was moving a $-I$ chromatic correction module in the vertical plane from the congested interaction region into the nearby arcs. In the horizontal plane, we kept the $-I$ module immediately after the final focusing quadrupoles since the dipole for separating the beams near the IP provides dispersion naturally. However, the additional dipole needed to make dispersion symmetric inside the $-I$ section was removed in order to resolve the problems of interference between the magnets in the LER and the HER. At first, the asymmetry of dispersion at the first pair of sextupoles did not cause any degradation of the dynamic aperture. Therefore, the new lattice was adopted as the official design[2].

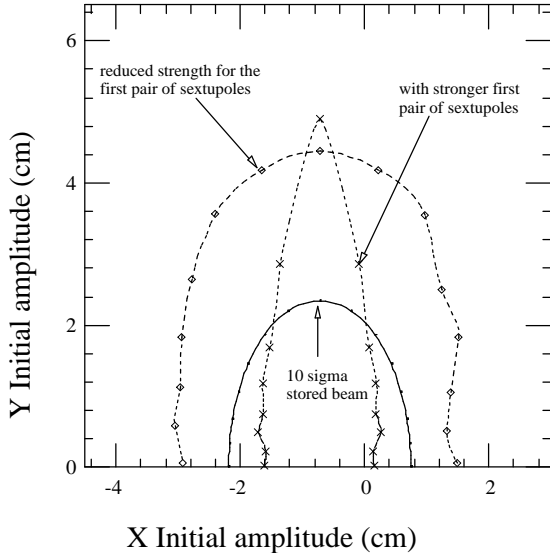


Figure 1: Dynamic apertures for ideal LER lattices with $10\sigma_E$ synchrotron oscillation

A month later, we made another change in the optics in two wiggler sections to accommodate a new wiggler configuration. We were surprised to see that the dynamic aperture(Fig. 1) dropped below 10σ in the horizontal plane even

for the case without any imperfections of alignment and multipole.

We calculated the effective Hamiltonian introduced in the last section and saw that the term $x\delta^2$ increased significantly from the previous lattice. Knowing this large second order dispersion in the one-turn map, it was not hard to figure out where it was generated in the lattice. Indeed, one could show that the asymmetry of dispersion at the pair of sextupoles separated by $-I$ would be the source of the second order dispersion. Using the method of paper[7], we could derive a combined map for the pair of sextupoles from

$$e^{-\frac{1}{3!}K_S:(x+\eta_1\delta)^3} e^{-\frac{1}{3!}K_S:(-x+\eta_2\delta)^3} \approx e^{-\frac{1}{3!}K_S:(3(\eta_1+\eta_2)x^2\delta+3(\eta_1^2-\eta_2^2)x\delta^2+(\eta_1^3+\eta_2^3)\delta^3)}, \quad (4)$$

where K_S was the strength of the sextupoles, x was the horizontal coordinate, and η_1 and η_2 were the dispersions at the positions of the first and second sextupoles respectively. In the derivation, we first transported the map of the second sextupole to the place near the first sextupole by a similarity transformation, then used the first order approximation of the Cambell-Baker-Hausdorff theorem to concatenate the maps. Additionally, the derivation itself showed us another method to obtain the effective Hamiltonian without going through a Taylor map. It was obvious from the result that the second order dispersion $x\delta^2$ was due to the difference in the dispersions.

We were then ready to explain why the dynamic aperture degraded for the last modified lattice. Since the non-linear dispersion was propagated in the lattice according to the betatron phase, a localized source, as we discussed earlier, may not be a problem if it reached its minimum value at the location of a RF cavity where the synchrotron and betatron oscillations were coupled. Fortunately, that was the case before wiggler sections were modified. It became the opposite with a maximum value of non-linear dispersion at the RF cavity after the modification.

It was clear from Eq. 4 that the second order dispersion was proportional to the strength of the sextupoles. Based upon this observation, we started to search for a chromatic solution in which the strength of the first horizontal pair of sextupoles was minimized. Once we found a such solution, the dynamic aperture recovered back above 10σ as shown in Figure 1.

4 SYNCHROTRON SIDEBANDS

In the conceptual design report[1], the tunes for the HER lattice were selected as $\mu_x = 0.57$ and $\mu_y = 0.64$ based solely on the simulation of the beam-beam effects. The selected tunes worked just as well for the lattice with the nominal $\beta_y^* = 2.0$ cm.

But when we tried to reduce the β_y^* from 2.0 to 1.5 and then to 1.0 cm the lattice became very sensitive to any imperfections. Again we checked with the effective Hamiltonian for the clues. Its coefficients normalized at 10σ of beam size were plotted in Fig. 2. From the figure, we could

see that the terms $x^2\delta$ was the largest among all the coefficients in the Hamiltonian. This term along with the term $x^2\delta^3$ drove the synchro-betatron resonance of $2\mu_x - 3\mu_s = 2 \times 0.57 - 3 \times 0.05207 = 0.984$. The reason for the sensitivity of the lattices was the fact of that this half integer synchrotron sideband was too close to the horizontal tune.

Actually we had demonstrated that it was the source of the problem by simply taking out this term in the map and tracking with the modified map to see if the dynamic aperture was better. Of course, it was positively identified.

In this case, we only made a change in working tunes $\mu_x = 0.618$ and $\mu_y = 0.638$ to avoid the sideband. After the change, we were able to achieve the $\beta_y^* = 1.0$ cm, which equals to the bunch length of the beams. The improvement of the lattice provided us more flexibility in optimization of the luminosity.

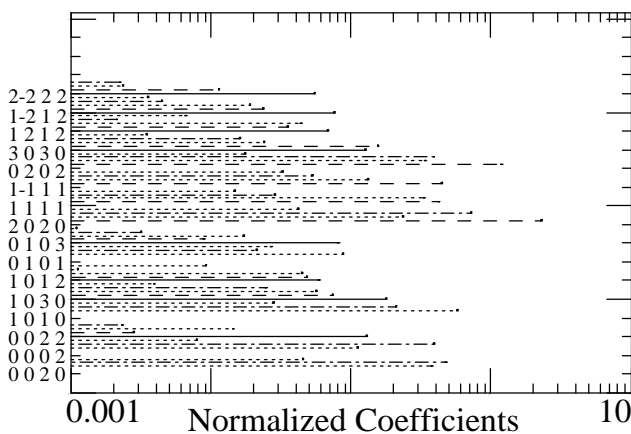


Figure 2: Normalized coefficients of the effective Hamiltonian plotted in log scale horizontally. The vertical axis shows corresponding indices (m_x, m_y, n_x, n_y) for resonances and orders. The corresponding chromatic indices, p's, are not explicitly shown but are indicated with line patterns (p = 0: solid, 1: dashes, 2: dots, 3: dotdashes, etc.)

5 CHROMATIC COUPLING

A scheme of solenoid compensation[8] was worked out for the LER a year ago. Among skew quadrupoles used, there were two pairs of skew quadrupoles located near the sextupoles separated in $-I$ in the arcs adjacent to the interaction region mainly to correct and adjust the vertical dispersion. Those skew quadrupoles were purposely placed outside of the pair of sextupoles so that the symmetry in the $-I$ section would be preserved. Recently, two of the skew quadrupoles were moved to the other side of sextupoles because it was a simple engineering solution to avoid the bigger vacuum pipe. Once again, the symmetry in the $-I$ module was broken. We saw a big chromatic coupling term $xy\delta$ in the Hamiltonian. The dynamic aperture was deteriorated as well. One could commute the map of the skew quadrupole with the map of sextupole in a different phase using the CBH theorem. The $xy\delta$ term would be generated

as a result. The resolution of this problem was to avoid any engineering solution with skewquadrupoles between paired sextupoles.

6 SUMMARY

From the examples discussed in previous sections, we can see that Lie algebra techniques were routinely and successfully used in the design process for the PEP-II lattices, especially for diagnosing non-linear aberrations. We found that the concept of the effective Hamiltonian was particularly useful since it contained a minimum set of coefficients and all the important information related to single particle dynamics, such as chromaticity, and strength of resonances. It also provides us an alternate way of thinking of an accelerator as an effective Hamiltonian combined from a sequence of hamiltonians rather than a sequence of electromagnetic elements.

7 REFERENCES

- [1] "PEP-II: An Asymmetric B Factory," Conceptual Design Report, SLAC-418, June 1993.
- [2] Y. Cai *et al.*, "Low Energy Ring Lattice of the PEP-II Asymmetric B-Factory," Proc. of 1995 Particle Accelerator Conference, Dallas, May 1995.
- [3] M.H.R. Donald *et al.*, "Lattice Design for the High Energy Ring of the SLAC B-Factory (PEP-II)", Proc. of 1995 Particle Accelerator Conference, Dallas, May 1995.
- [4] M. Berz, "Differential Algebraic Description of Beam Dynamics to Very High Orders", Particle Accelerators, Vol. 24 p109, 1989.
- [5] Y.T. Yan, J. Irwin, and T. Chen, "Resonance Basis Maps and nPB Tracking for Dynamic Aperture Studies", Proc. of 1995 LHC workshop, Montreux, October, 1995.
- [6] A.J. Dragt, in Physics of High-Energy Particle Accelerators, AIP Conf. Proc. No. 87, edited by R.A. Carrigan *et al.*(AIP, New York, 1982)
- [7] John Irwin, "The Application of Lie Algebra Techniques to Beam Transport Design", SLAC-PUB-5315, August 1990.
- [8] Y. Nosochkov, Y. Cai, J. Irwin, M. Sullivan, E. Forest, "Detector Solenoid Compensation in the PEP-II B-Factory," Proc. of 1995 Particle Accelerator, Dallas, May 1995.